For the aviation sector, it is extremely important to devise revolutionary solutions in the field of technology to restrain the potential impact of civil aviation on the environment to the level of the established strategic goals of ACARE (FlightPath2050). The introduction of innovative technologies (improvement of the combustion chamber, the introduction of electric hybrid power plants on airplanes, and the use of alternative aviation fuel) will ensure the sustainable growth of air transportation.

To assess the effectiveness of advanced technologies, it is extremely important to have a model for calculating global/local emissions that takes into account the parameters of the flight path of conventional and hybrid aircraft, operational characteristics of the aircraft engine and hybrid powerplant, and the features of sustainable fuel.

The improved module for calculating emission indices by combining the module for calculating the parameters of the flight path and the results of calculating the thermogas-dynamic calculation of the aircraft engine makes it possible to detect the influence of fuel consumption (engine thrust) on the values of the emission indices. This feature is representative for evaluating the efficiency of hybrid powerplants because the electrification of the aircraft fleet is primarily aimed at reducing fuel consumption.

The analysis of simulation results reveals that the fuel consumption and EINOx are significantly reduced (for the climb stage – 25 %; for the descent stage – 30 %) for the hybrid AN26 compared to the conventional AN26. The specified operational measure, in the part of the low-pitch descend, significantly reduces EICO for the hybrid AN26 by an average of 50 % compared to the descend stage for the conventional trajectory.

The results of calculations for the entire flight path demonstrate that the use of a hybrid power plant for An26 contributes to an average reduction of fuel consumption by 10 %, NO_x emissions by 25 %, water vapor emissions by 10 %, and CO_2 by 10 %

Keywords: pollutant emission, flight trajectory simulation, hybrid power plant

UDC 504.06: 629.735.018.7.07:656.71(045)
DOI: 10.15587/1729-4061.2024.302793

IMPROVING THE CALCULATION MODULE FOR ESTIMATING POLLUTANT EMISSION FROM CONVENTIONAL AND HYBRID REGIONAL AIRCRAFT

Kateryna Synylo
Corresponding author
PhD, Associate Professor*
E-mail: synyka@gmail.com
Vitalii Makarenko
PhD**
Andrii Krupko
Postgraduate Student*
Vadim Tokarev
Doctor of Technical Sciences**
*Department Civil and Industrial Safety***
Scientific Research Department*
***National Aviation University
Lubomyra Huzara ave., 1, Kyiv, Ukraine, 03058

Received date 12.02.2024
Accepted date 18.04.2024
Published date 30.04.2024

How to Cite: *Synylo, K., Makarenko, V., Krupko, A,. Tokarev, V. (2024). Improving the calculation module for estimating pollutant emission from conventional and hybrid regional aircraft. Eastern-European Journal of Enterprise Technologies, 2 (10 (128)), 34–44. https://doi.org/10.15587/1729-4061.2024.302793*

1. Introduction

Over the past 40 years, aviation has become a powerful driver of economic and social development, creating around 62.7 million jobs (equivalent to the size of the UK population) and USD 2.7 trillion in global economic activity, representing 3.6 % of global GDP [1]. Until 2019, the growth prospects of the aviation sector were quite optimistic. Recent estimates by aircraft manufacturers (Boeing [2], Airbus [3], Bombardier, etc.) predicted an increase in air travel demand of 4.3 % per year over the next 20 years.

The COVID-19 pandemic has had a significant impact on the aviation industry due to travel restrictions and reduced demand for air travel. Global passenger traffic has experienced an unprecedented decline in history, with a total reduction of more than 2.7 billion passengers (–60 %) in 2020 compared to the level of 2019 [4]. An analysis of air transport growth trends until 2050 under various scenarios demonstrates the recovery of global demand for passenger, cargo, and business class air transport. Achieving the volume of air transport at the level of 2019 was already expected in 2023, 2024, and 2027, respectively, for the scenario with high, medium, and low intensity, Fig. 2 [5].

To ensure the sustainable growth of the aviation sector, it is extremely important to devise revolutionary solutions in the field of innovative technologies to contain the potential impact of civil aviation on the environment to the level of the established strategic goals of ACARE (FlightPath2050) [6–8]:

– goal No. 9 is aimed at achieving emission targets, taking into account the use of advanced technologies, in particular the improvement of the combustion chamber [6];

– goal No. 10 refers to the introduction of electric hybrid propulsion systems (PS) on airplanes and is aimed at radical changes in the airport infrastructure due to battery charging requirements [6];

– goal No. 12 is aimed at the use of alternative aviation fuel to reduce global and local emissions [6].

Innovative technologies and focused efforts in R&D are essential to ensure the sustainable growth of air transport. ACARE will continue to promote the need to monitor achievement and progress towards strategic goals [4, 5].

Fig. 1 shows trends in global CO_2 emissions, including future forecasts under various scenarios of air transportation, innovative technologies, and air traffic management [7].

Compared to 2019, in 2020 the share of aviation NO_X emissions in the transport sector fell from 22.8 % to 13.4 %, while the share of total NO_X emissions almost halved from 10.6% to 6 % [7].

Fig. 2 shows trends in NO_X emissions, including future forecasts under various air transport scenarios, innovative technologies, and air traffic management [7].

For the baseline scenario, the most optimistic technology and air traffic management scenario would bring NO_X emissions closer to 2019 levels in 2050. The same applies to CO and volatile PM emissions, while HC and non-volatile PM emissions may decrease between 2019 and 2050.

An analysis of air transport growth trends to 2050 indicates that technology alone will not be sufficient to achieve the required aviation emission reductions in line with Flightpath 2050 targets. An integrated systems approach is essential, combining hybrid electric solutions for regional aircraft with an engine adapted to green aviation fuels (SAF) or for long-haul hydrogen-powered aircraft. The synergy of ambitious low-emission technologies and SAF adaptation implies a 90 % improvement in carbon efficiency by 2050 compared to today's aircraft fleet.

To evaluate the effectiveness of advanced technologies, the construction of a model for calculating global/local emissions that takes into account the parameters of the flight path of conventional and hybrid aircraft, operational characteristics of the aircraft engine and hybrid powerplant, as well as features of sustainable fuel, is relevant.

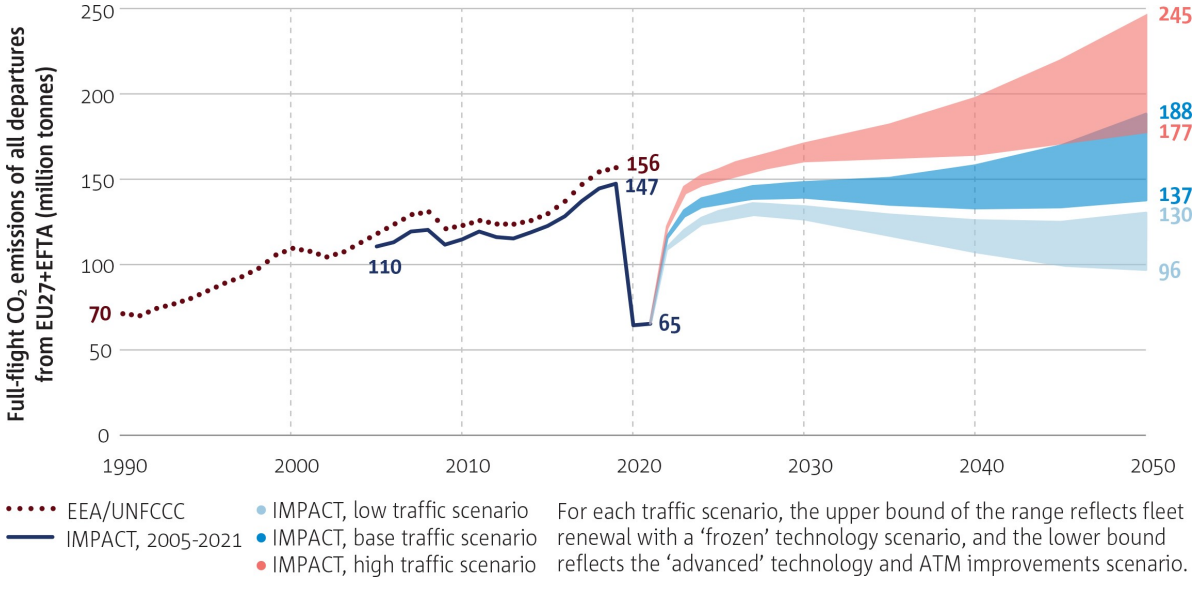

Fig. 1. Trends in global aviation CO_2 emissions for different scenarios [7]

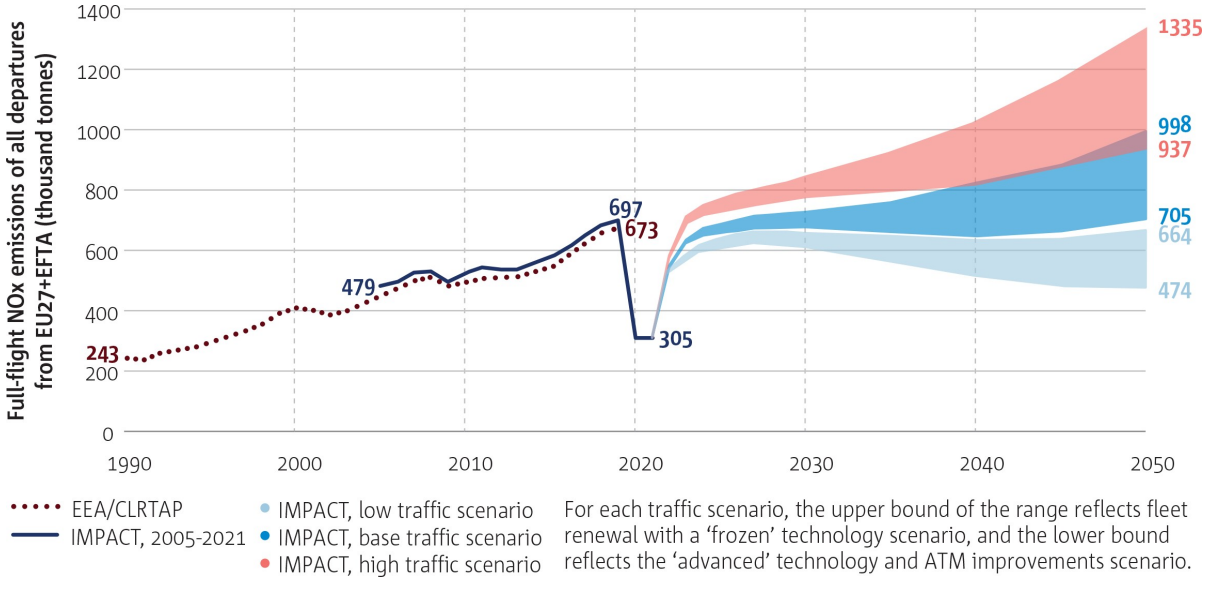

Fig. 2. Aviation NOx emission trends for different scenarios [7]

2. Literature review and problem statement

Aircraft engine (AE) emission is the main factor of atmospheric air pollution (AP) both in the lower atmosphere and in the upper atmosphere (cruising flight).

The results of research on the inventory of airport pollution sources [5] indicate that emissions during the operation of aircraft in the airport area make up 97.3 % of the total mass of emissions during the take-off and landing cycle (TLC) are hydrocarbons. At the same time, 94.3 % of CO occurs during the taxiing stages of the aircraft before takeoff and after landing, taking into account the period of start-up and warm-up of AE [5]. Also, the results of study [5] indicate that emissions of nitrogen oxides of AE during TLC period are divided into take-off, altitude gain, landing and low throttle modes and are, respectively, 26.7 %, 53.6 %, 10.5 %, and 9,2 % of the total mass of NOx emission over TLC. Therefore, aircraft are the dominant source of pollution in the airport area. The revealed trends in work [7] demonstrate that the intensity of the emission of aircraft depends on the type and mode of operation of AE, their number in the power plant, the speed and direction of movement of the aircraft, as well as on a number of other operational factors.

In Ukraine, the assessment of atmospheric air pollution as a result of the emission of aircraft engines during the operation of aircraft in the airport area is carried out according to the current regulatory methodology OND-86. The approach of this procedure does not take into account the operating conditions of the aircraft, in particular, movement within the airfield at different speeds, as well as the layout of AE on the aircraft and other factors. According to this procedure, the size of the sanitary protection zone of the airport is determined on the basis of calculations for stationary sources of emissions, while the extraction of the component of AE emissions from airport air pollution is inadmissible due to their predominance.

The ICAO manual on airport air quality control (ICAO Doc 9889) [8] offers three main methods for estimating air pollution (NOx, CO, and HC) emissions by the degree of accuracy and complexity of the calculation algorithm [9]: the ICAO method, the $BFFM_2$ method, and the P_3T_3 method.

The ICAO method is a fairly simple one as it is based on a rather elementary calculation scheme and is characterized by the availability of initial data provided by the ICAO bank. As shown in ICAO Doc 9889 [8], this method can only be used to calculate emissions specific to each mode of the take-off and landing cycle. But we should point out the low level of accuracy of this method. ICAO Doc 9889 [8] also points out a limitation of the ICAO method for cruise mode, which will require interpolation between ICAO standard power parameters (7 %, 30 %, 85 %, and 100 %), which will typically require a non-linear curve fit between EI and fuel flows. Therefore, the ICAO method is not advisable to use for operational conditions outside the take-off and landing cycle. Instead, higher accuracy methods such as the P_3T_3 and $BFFM_2$ method should be used.

The $BFFM_2$ method is an average one in terms of the complexity of the calculation schemes and the availability of the necessary initial data. In [10], it is emphasized that the emission indices calculated by the $BFFM_2$ method are characterized by a high level of accuracy, while at the same time some uncertainties are indicated, which should be included in the part of the refinement of the predicted emission indices.

Studies [11, 12] indicate some difficulties in calculating HC and CO, in particular for traction less than 7 %, since the recalculation of EIHC, EICO for standard conditions can get unrealistically high values.

The P_3T_3 method contains a fairly complex calculation algorithm and requires a number of initial data, the availability of which is often limited by the confidentiality and ownership of AE manufacturer. These are, in particular, the pressure (P_3) and temperature (T_3) at the entrance to the AE combustion chamber. In work [10] it is emphasized that the P_3T_3 method for estimating AE emission indices is characterized by high accuracy, but the implementation of this method is complicated not so much by the laboriousness of the calculation algorithm as by the unavailability of initial data. This problem is solved within the framework of international projects by independent calculation of pressure (P_3) and temperature (T_3) at the entrance to the combustion chamber according to the thermogas-dynamic calculation equations for AE.

Research results [13] demonstrate the limitations of the P_3T_3 method for turboprop engines. The accuracy of NOx estimates using the recommended pressure exponents is estimated to be ±11 %, for a given P_3 and T_3 under standard conditions.

Paper [14] presents a comparison of the results of the AE EI_{NOx} assessment at different altitudes according to the considered methods ($BFFM_2$ and P_3T_3). The difference between the results of the specified models increases with height. The observation is caused by the influence of AP humidity on the value of EI_{NOx}.

The $BFFM_2$ method is used not only to estimate cruise emissions but also to estimate the total amount of pollutants emitted by the aircraft during the entire baseline flight. This method is also used to support the creation of a 3D emission inventory and subsequent assessment of the impact of aviation on climate change.

Therefore, the considered methods ($BFFM_2$ and P_3T_3) are characterized by high accuracy, but their application is complicated by the unavailability of initial data (fuel consumption, P_3, T_3). An option to overcome the difficulties may be to combine the module for calculating the parameters of the flight path, the module for thermogas-dynamic calculation of the aircraft engine, and the module for calculating the emission indices.

3. The aim and objectives of the study

The purpose of our study is to improve the module for calculating the emission indices of the aircraft engine under real operational and meteorological conditions, which makes it possible to improve the procedure of inventorying aircraft engine emissions and to identify the contribution of aircraft emissions to global, regional, and local atmospheric air pollution.

To achieve the goal, the following tasks were solved:

– to calculate the parameters of the flight path (altitude, Mach number, speed of the aircraft) of a conventional or hybrid aircraft;

– to substantiate emission indices at ICAO certification points for an aircraft with a hybrid power plant;

– to simulate emission indices for aircraft with conventional and hybrid power plants taking into account real fuel consumption along the flight path.

4. The study materials and methods

The object of our study is AE emission, which is a function of thermodynamic parameters (temperature in the combustion chamber and the degree of pressure change in the compressor), which in turn depend on the temperature, pressure, and humidity of AP.

In the course of the study, the hypothesis was tested that as a result of the modernization of the power plant of the An-26 aircraft by using an electric engine in it, there could be a reduction in fuel consumption and a reduction in PS emissions.

The main methods for estimating mass emissions (inventory) of hazardous PS from AE are based on the following formula:

$$Q = FF \times EI \times T \times n, \quad (1)$$

where Q is pollutant emission; FF – fuel consumption indicator, kg/s; EI – emission index, g/kg; T – time of operation (work) of AE, s; n is the number of engines on aircraft.

The $BFFM_2$ method is aimed at estimating the emission indices (NOx, CO, and HC) of AE and the fuel consumption index for real operational and meteorological conditions [9, 10]. The key components of the method are semi-empirical approaches for adjusting atmospheric conditions and establishing the relationship between EI and fuel consumption. Therefore, it is sufficient to determine the actual fuel consumption based on the model or measurement (for a specific segment of the flight profile) to predict the emission value for these operating conditions. Data and results corresponding to flight conditions are designated as "non-reference" values, while fuel consumption and emission indices from the ICAO database are "reference" values. This is due to the fact that the latter correspond to the conditions of the International Standard Atmosphere (ISA) at sea level.

First, on the basis of data from the ICAO bank for four basic thrust modes of the studied AE type (7 %, 30 %, 85 %, 100 %) plots of EI_{NOx}, EI_{CO}, EI_{HC} dependences on the fuel consumption indicator are constructed in a logarithmic scale for conditions of ISA, Fig. 3.

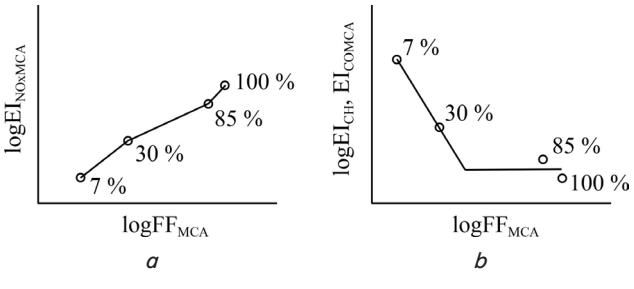

Fig. 3. Principles of determining emission indices from fuel consumption according to ICAO bank data: *a* – EI_{NOx}; *b* – EI_{CO}, EI_{HC}

Second, real meteorological conditions (temperature, pressure, and humidity of AP) are converted into ISA conditions according to the formulas for adjusting humidity and pressure [10, 11].

Correction of air temperature (θ) and atmospheric pressure (δ):

$$\theta = \frac{T_0}{288.15}, \quad (2)$$

where T_0 – ambient air temperature, K;

$$\delta = \frac{P_0}{101{,}325}, \quad (3)$$

where P_0 is atmospheric pressure, Pa;

Correction of AP humidity, which significantly affects EI_{NO_x}, EI_{CO}, EI_{HC}:

$$H = -19.0 \times (\omega - 0.00634), \quad (4)$$

where ω – specific humidity:

$$\omega = \frac{0.62197058 \times RH \times P_{SAT}}{(P_{psia} \times 68.9473) - (RH \times P_{SAT})}, \quad (5)$$

where RH is relative humidity; P_{SAT} – saturated vapor pressure in millibars; P_{psia} – atmospheric pressure in units of measurement, pounds/m^2.

The actual fuel consumption indicator is adjusted relative to ISA according to the following calculation formula:

$$FF_{ISA} = \frac{FF}{\delta_{amb}} \times \theta_{amb}^{3.8} \times e^{0.2 \times M^2}, \quad (6)$$

where δ_{amb} is the ratio of the atmospheric pressure adjusted to the conditions of ISA; θ_{amb} – the ratio of AP temperature adjusted to the conditions of ISA; FF – actual fuel consumption, kg/s; M is the Mach number.

The corresponding referents values $EI_{NO_x\,ISA}$, EI_{COMCA}, EI_{HCMCA} are determined by the method of linear interpolation based on the calculated value of fuel consumption on the basis of the typical dependences constructed above according to the data of the ICAO bank for the investigated type of AE.

Equations (6) are used to convert fuel consumption and EI values from non-reference conditions to reference conditions. The reference fuel consumption and emission index EI are obtained from the ICAO database, while the fuel consumption and Mach number associated with the flight segment are obtained from the aircraft performance model or from measurement.

The found reference values $EI_{NO_x\,ISA}$, $EI_{CO\ ISA}$, $EI_{HC\ ISA}$ for the conditions of ISA are converted into real meteorological conditions:

$$EI_{NO_x} = EI_{NO_x\,ISA} \times e^{H} \times \left(\frac{\delta^{1.02}}{\theta^{3.3}}\right)^{x}, \quad (7)$$

$$EI_{HC} = EI_{HC\ ISA} \times \left(\frac{\theta^{3.3}}{\delta^{1.02}}\right)^{x}, \quad (8)$$

$$EI_{CO} = EI_{CO\ ISA} \times \left(\frac{\theta^{3.3}}{\delta^{1.02}}\right)^{x}, \quad (9)$$

where $EI_{NO_x\,ISA}$, $EI_{CO\ ISA}$, $EI_{HC\ ISA}$ are emission indices determined by the certification curve according to ICAO bank data.

The specified method also allows taking into account the influence of meteorological conditions (temperature, pressure, humidity) at the corresponding height of the profile segment.

The algorithm for modeling emission indices using the $BFFM_2$ method, taking into account the necessary initial data, is shown in Fig. 4.

The error of estimating EI_{NO_x}, EI_{CO}, EI_{HC} for aircraft engines by the presented method is ±10 % with a standard deviation of 6 % and is caused by the following factors [13]:

– the accuracy of the linear interpolation method for determining the emission index according to the certification curve is significantly reduced for the operational modes of the investigated type of AE with a thrust index of less than 7 %;

– AE operation period;

– lack of information for some types of AE.

The PolEmiCa complex model (developed at NAU in 2013, verified at CAEP/ICAO in 2020) implements the $BFFM_2$ method for calculating emission indices (Fig. 4, 5).

To perform the research tasks for the conventional and hybrid turboprop engine, the module for calculating the emission indices based on the $BFFM_2$ method was improved. This module takes into account flight path parameters (altitude, Mach number, aircraft speed), operational parameters (real fuel consumption) and meteorological conditions (humidity, temperature, atmospheric pressure), Fig. 5.

It should be emphasized that the presented emission index evaluation module provides objective initial data for the inventory of aircraft engine emissions and further modeling of the processes of transfer and dilution of impurities by the jet of exhaust gases from the aircraft engine and atmospheric turbulence.

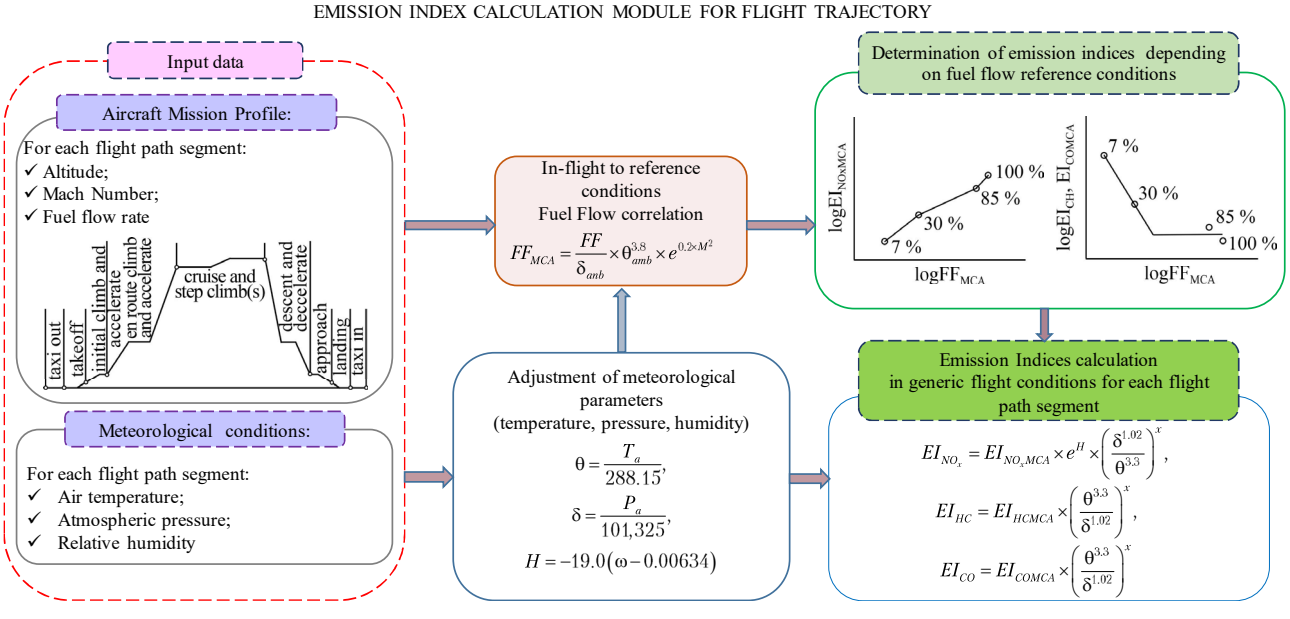

Fig. 4. Main elements of modeling emission indices using the $BFFM_2$ method

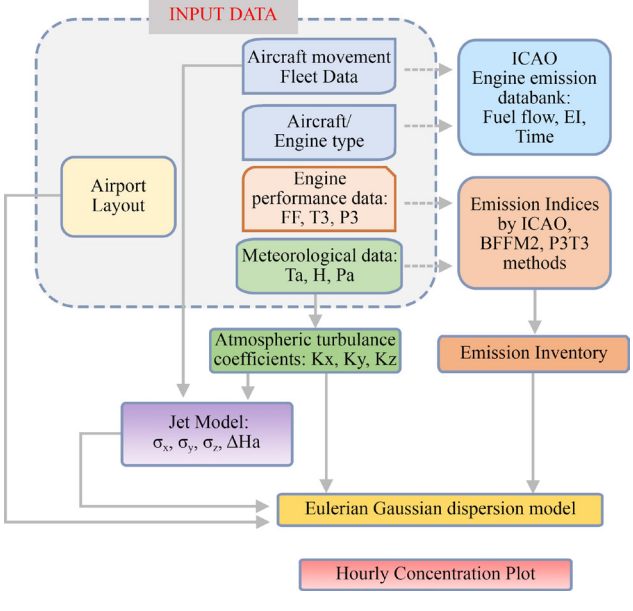

Fig. 5. PolEmiCa integrated model: calculation of emissions and levels of atmospheric air pollution due to aircraft emissions: vertical and horizontal dispersion of the jet – σ_x; σ_y; σ_z; ΔH is the height of the rise of the jet of gases from the aircraft engine; Ta – atmospheric air temperature, K; H – humidity, %; Pa – atmospheric air temperature, Pa; Kx, Ky, Kz – horizontal and vertical coefficients of atmospheric turbulence

5. Results of the study on calculating the emission indices of turboprop engine under real operating and meteorological conditions

5. 1. Calculation of flight path parameters for a conventional or hybrid aircraft

The calculation of the flight trajectory was based on the solution of a system of ordinary differential equations, which describe the flight of an airplane as the movement of a material point of variable mass in a vertical plane under the influence of the forces of gravity W, thrust T, drag D, and lift force L. To simplify the complex dynamics of flight, a number of assumptions was used: the Earth is flat, there is no wind, the acceleration of Earth's gravity g is constant:

$$\begin{cases} \frac{dv}{dt} = \frac{1}{m}\left(T\cos\varepsilon - D - W\sin\theta\right), \\ \frac{d\theta}{dt} = \frac{1}{mv}\left(T\sin\varepsilon + L - W\cos\theta\right), \\ \frac{dh}{dt} = v\sin\theta, \\ \frac{dx}{dt} = v\cos\theta, \\ \frac{dm}{dt} = -G, \end{cases} \quad (10)$$

where v is the flight speed, t is the flight time, m is the mass of the aircraft at the moment of time t, $\varepsilon=\alpha+\beta$, α is the angle of attack, β is the angle of installation of the engines in relation to the wing centerline chord, θ is the trajectory angle, h is geometric height of the flight, x is the length of the projection of the flight profile on the horizontal plane from the beginning of the flight segment, G is the total fuel consumption at the moment of time t. Drag is determined from the following equation:

$$D = c_x \frac{\rho v^2 S}{2}, \quad (11)$$

where c_x is the drag coefficient, ρ is the air density, S is the wing area.

The lift force is determined in a similar way:

$$L = c_y \frac{\rho v^2 S}{2}, \quad (12)$$

where c_y is the lift force coefficient.

Given the fact that the accepted assumptions equally affect both the aircraft with a conventional PS and the aircraft with a hybrid PS, the proposed trajectory model should be sufficient for the comparison of emission characteristics. To confirm the effectiveness of hybridization, calculations were performed on the example of the An-26 aircraft with conventional and hybrid PSs. That is, two AI-24VT engines and one RU-19-300 were replaced by two TV3-117VMA-SBM1 with reduced power and 2 electric motors.

The thrust calculation was based on modeling the gas-dynamic process of the engines and the power of the electric motor in accordance with the instructions in book [15]. When modeling a hybrid aircraft, a parallel PS architecture was used [16]. As a result of the simulation, the dependence of power on the propeller shaft and fuel consumption on altitude and flight speed for an aircraft with a hybrid PS was obtained. The height-speed characteristics of the thrust of the propeller are obtained on the basis of the drive disk theory. Together with the power on the propeller shaft, this has made it possible to establish the dependence of thrust of the hybrid PS on altitude and speed.

Trajectories were calculated in full compliance with the An-26 flight operation manual for both the conventional and hybrid versions of the aircraft, because the aerodynamics of the aircraft remained unchanged. The maximum take-off weight of 24 tons was used for the simulation. The excess weight associated with the installation of additional batteries, electric motors, gearboxes, modernization of the exhaust system, cooling and communication was subtracted from the fuel weight without reducing the payload. The trajectory calculation was performed for storage batteries with a specific capacity of 435 W·h/kg, the development of which is predicted in the future. Since at different stages of the flight, the flight operation manual provides for different restrictions, according to them, the trajectory is divided into segments (Table 1). For each of these segments, the system of differential equations was solved separately with the initial values of v, θ, h, m taken from the end of the previous segment.

In order to ensure the safety of the aircraft flights along the calculated trajectories, the requirements of the An-26 flight operation manual were met. These requirements are formulated in the form of multipliers of the objective function k_i (Table 2):

$$\min \prod k_i.$$

The aircraft flight profile calculation method has been improved by using a genetic algorithm (GA) to satisfy multiple operational constraints simultaneously. A separate optimization was performed on each flight segment. The optimization was carried out using parameters of the function of the angle of attack α versus time and parameters of the function of the power lever angle versus time.

Table 1

Description of flight path segments

Segment	No.
Run-up in take-off mode	1
Gaining speed during a flight separated from the ground by the poles near the ground	2
Gaining altitude at a safe speed over the poles near the ground	3
Set speed up to 240 km/h at the poles far from the earth	4
Lifting the chassis	5
Set speed up to 280 km/h and a height of 150 m	6
Closing the flaps and speed up to 310 km/h	7
Height gain up to 5.8 km	8
Deduction of the trajectory angle to zero, height gain up to 6 km	9
Cruise flight	10
Descent to a height of 4.5 km	11
Release of flaps by 15 degrees in pulses of 5 degrees and output to a speed of 310 km/h	12
Chassis release	12
Speed reduction to 240 km/h	12
Release flaps to 38 degrees in pulses of 5.75 degrees and output to a speed of 210 km/h	13
Descent to about 100 m with access to the corner of the slope	14
Flight on the glissade	15

Table 2

Multipliers of the objective function to meet the conditions of the flight operations manual

No.	Multiplier of objective function	Purpose
1	$1+\lvert v_{1e}-v_1\rvert$, where v_{1e} – the velocity at the end of the segment obtained as a result of solving a system of differential equations; v_1 – planned speed at the end of the segment	To achieve velocity v_1 at the end of the segment
2	$\begin{cases}1 \text{ at } \max h \geq h_1,\\ 1+h_1-\max h \text{ at } \max h < h_1\end{cases}$	To reach/exceed height h_1
3	$\begin{cases}1 \text{ at } \min h \leq h_1,\\ 1+\min h-h_1 \text{ at } \min h > h_1\end{cases}$	To reach/descend below height h_1
4	$1-\sum_{\Delta v<0}\Delta v$, where $\Delta v_i=v_i-v_{i-1}$	To ensure a monotonous increase in speed
5	$1+\sum_{\Delta v>0}\Delta v$, where $\Delta v_i=v_i-v_{i-1}$	To ensure a monotonous decrease in speed
6	$1-\sum_{\Delta h<0}\Delta h$, where $\Delta v_i=v_i-v_{i-1}$	To ensure a monotonous increase in height
7	$1+\sum_{\Delta h>0}\Delta h$, where $\Delta v_i=v_i-v_{i-1}$	To ensure a monotonous decrease in height
8	$\left(1+\sum \text{isnan}\, v\right)\left(1+\sum \text{isnan}\, h\right)$, where isnan is a function that determines whether a value is non-numeric, and v and h are one-dimensional arrays resulting from the solution of a system of differential equations	To increase the value of the objective function for solutions of a system of equations that do not make sense
9	$1+\lvert\theta\rvert$	To bring the trajectory angle to zero
10	$\begin{cases}1+t_1-t_{1e} \text{ at } t_{1e} < t_1,\\ 1+t_{1e}-t_2 \text{ at } t_{1e} > t_2,\\ 1 \text{ at } t_1 \leq t_{1e} \leq t_2,\end{cases}$ where t_{1e} – the end time of the segment, for example, the time it takes to reach the desired speed	To ensure the duration of the segment in the range from t_1 to t_2
11	$\begin{cases}1 \text{ at } v_{1e} < v_1,\\ 1+v_{1e}-v_1 \text{ at } v_{1e} \geq v_1\end{cases}$	To ensure that the velocity at the end of the segment is slower than the velocity v_{1e}
12	$1+\lvert m_{1e}-m_1\rvert$, where m_{1e} – aircraft weight at the end of the segment	To achieve the aircraft mass m_1 at the end of the segment
13	$1+\sum_{t<t_1 \wedge t>t_1-5}\lvert v(t)-v_1\rvert$	To hold speed for the last 5 seconds of segment

When using GA to estimate each value of the objective function (fitness function), the system of equations (10) was solved. The solution of this system of equations can be obtained using the MATLAB function "ode45". The need to use the global optimization algorithm is due to the non-linear dependence of the objective function on the parameters used to reduce the objective function.

In contrast to existing methods for calculating the flight path the improved method made it possible to fulfill the operational limitations and reliably predict the speed, altitude, fuel consumption, thrust, angle of inclination of the aircraft in the form of continuous functions of time throughout the flight profile. The presence of these functions is the basis for calculating the emission of pollutants.

The flight trajectory for the maximum range with contingency fuel reserve of 580 kg of fuel is shown in Fig. 6.

Fig. 6 demonstrates that at the same flight speed and flight altitude as the original An-26, the flight range of the updated PS increased by 11.7 %.

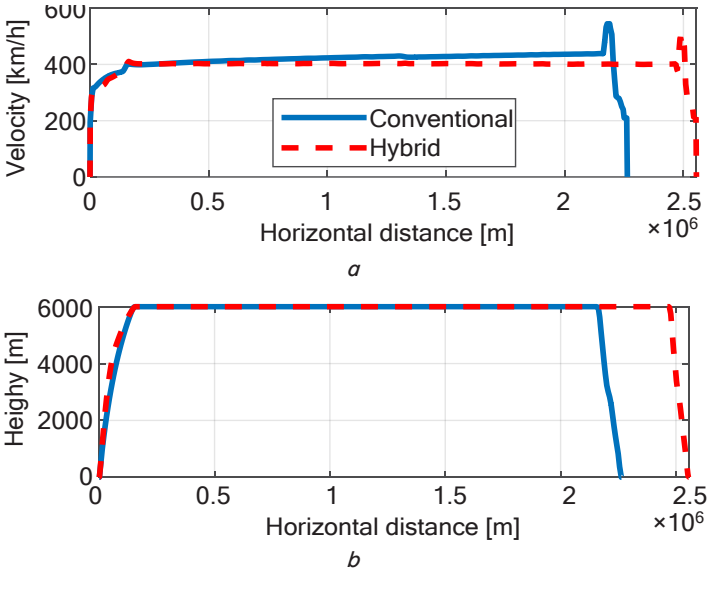

Fig. 6. Comparison of flight profiles of an aircraft with a conventional and hybrid power plant: *a* – true flight speed; *b* – geometric flight height

5. 2. Justification of the emission index at ICAO certification points for an aircraft with a hybrid power plant

For the developed model of PS with a hybrid power plant (similar to the TV3-117VMA-SBM1 with reduced power by 10 %), an analog was selected, taking into account the following factors:

– geometric configuration of PS;
– engine type: turboprop;
– number of engines: 2;
– engine power: 2250 hp.

The following types of engines were selected by type and power:

1. PW119B:
– $Ne._{tf}$=2282 hp (1678.11 kW);
– $Ce._{tf}$=0.220 kg/hp·h (0.299 kg/kW·h);
– N=1,796 hp (1320,96 kW);
– n_{tf}=1,300 rpm;
– M_{en}=415 kg.
Overhaul life – 4,000 hrs.
Application: Fairchild Dornier 328-110.
2. PW120:
– $Ne._{tf}$=2,100 hp (1,544.55 kW);
– $Ce._{tf}$=0.218 kg/hp·h (0.296 kg/kW·h);
– N=1,704 hp (1,253.29 kW);
– n_{tf}=1,200 rpm;
– M_{en}=417.8 kg.
Overhaul life – 8,000 hrs.
Application: DeHavillandDash 8-100 and Aerospatiale/AleniaATR 42-300/320.
3. PW125B:
– $Ne._{tf}$=2,626 hp (1,931.42 kW);
– $Ce._{tf}$=0.208 kg/hp·h (0.283 kg/kW·h);
– N=2,030 hp (1,493.07 kW);
– n_{tf}=1,200 rpm;
– M_{en}=481 kg.
Overhaul life – 8,000 hrs.
Application: Fokker 50.

Among the analyzed engine types and performed preliminary simulations, the PW125B installed on the Fokker 50 type aircraft was chosen as an analog for the AN26 type aircraft with a hybrid powerplant.

Fuel consumption and emission indices for the specified analog are given in the ICAO database, Table 3.

Table 3

Values of EINOx, EICO at ICAO points for the PW125B type engine

Mode	EINOx, g/kg	EICO, g/kg	FF, kg/s
T/F	18.095	2.09	0.1532
Climb	16.1	2.1	0.1351
Approach	10	3.5	0.0808
Taxi	6.89	9.195	0.0499

The typical dependences of EINOx, EICO for certification conditions built below allow us to determine EINOx, EICO for various operating conditions, Fig. 7, 8.

The specified dependences allow determining the emission index for critical values of fuel consumption (lower/higher than the specified values at the certification points) by interpolation, Fig. 7, 8.

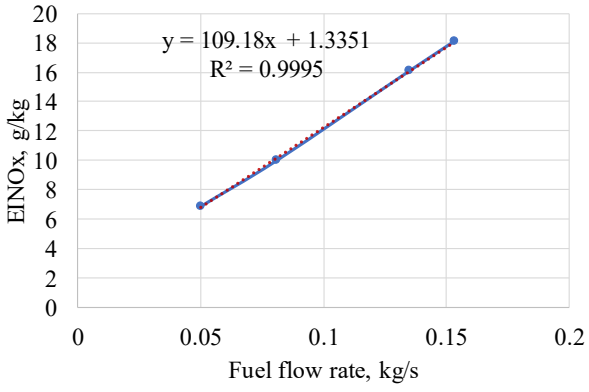

Fig. 7. Dependences of EINOx on fuel consumption at ICAO points (certification conditions)

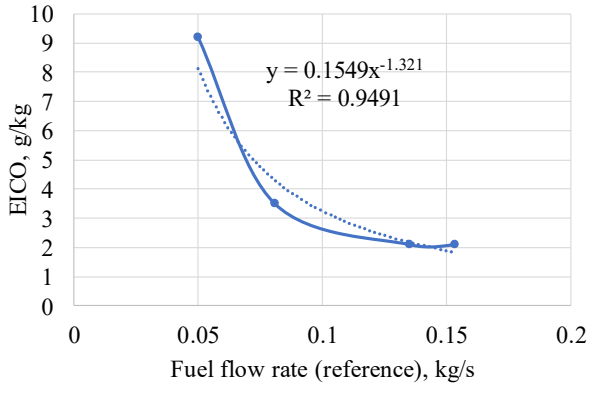

Fig. 8. Dependences of EICO on fuel consumption at ICAO points (certification conditions)

5. 3. Modeling of emission indices for an aircraft with conventional and hybrid power plants

For the calculation of EINOx, EICO, EICH for the AN26 type aircraft with conventional and hybrid power plants, operational and meteorological data were provided regarding:

1) flight trajectories (altitude, distance, speed, Mach number) of an aircraft with conventional and hybrid PS, Fig. 9, and Table 1;

2) the ratio of fuel and air in the combustion chamber of an aircraft engine;

3) meteorological parameters – temperature, humidity, and atmospheric pressure for the conditions of ISA.

The specified operational parameters were modeled on the basis of the module for calculating the flight profile of aircraft with conventional and hybrid PSs [17].

Modeling of emission indices for a conventional aircraft of the An26 type and a hybrid aircraft using the BFFM$_2$ method was performed for a classic trajectory and a trajectory with a low-pitch descent. The averaged EINOx, EICO for each segment of both types of flight path are shown, respectively, in Fig. 9, 10.

According to the PolEmiCa model, the mass values of burned fuel, emissions of NOx, CO, CO_2, and water vapor were determined for each segment of the trajectory (Fig. 11) of the flight for AN26 with a conventional and hybrid power plant.

The results of the calculation of the mass of PS emission showed that low-pitch descent makes it possible to reduce the mass of CO emission, but at the same time there is an increase in the mass of NOx, H_2O, CO_2 emission and fuel consumption.

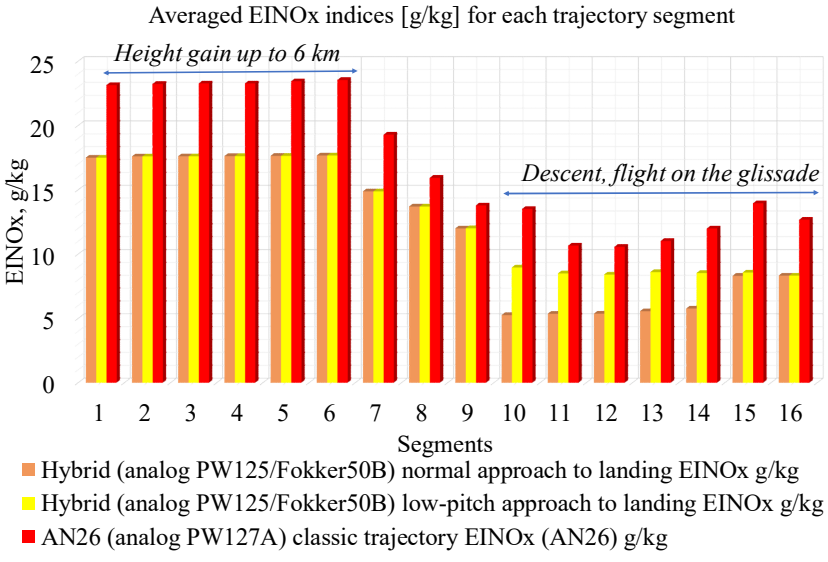

Fig. 9. Averaged EINOx indices [g/kg] for each trajectory segment of conventional and hybrid An26

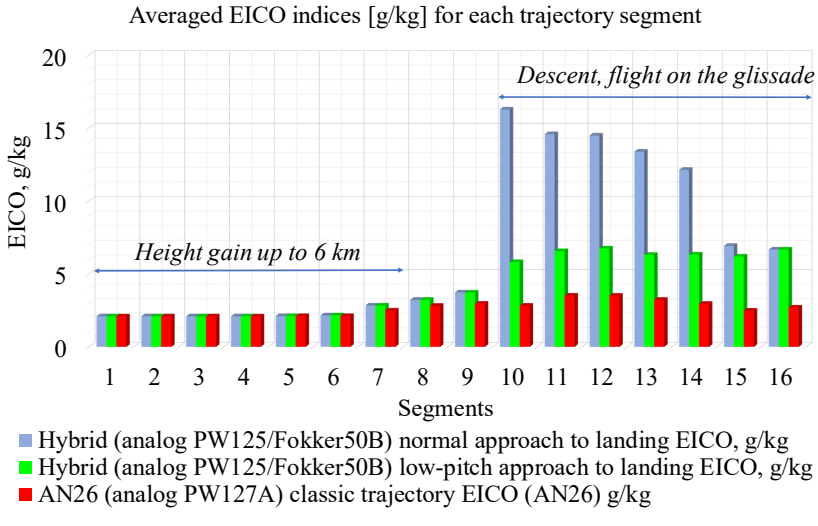

Fig. 10. Averaged EICO indices [g/kg] for each trajectory segment of conventional and hybrid An26

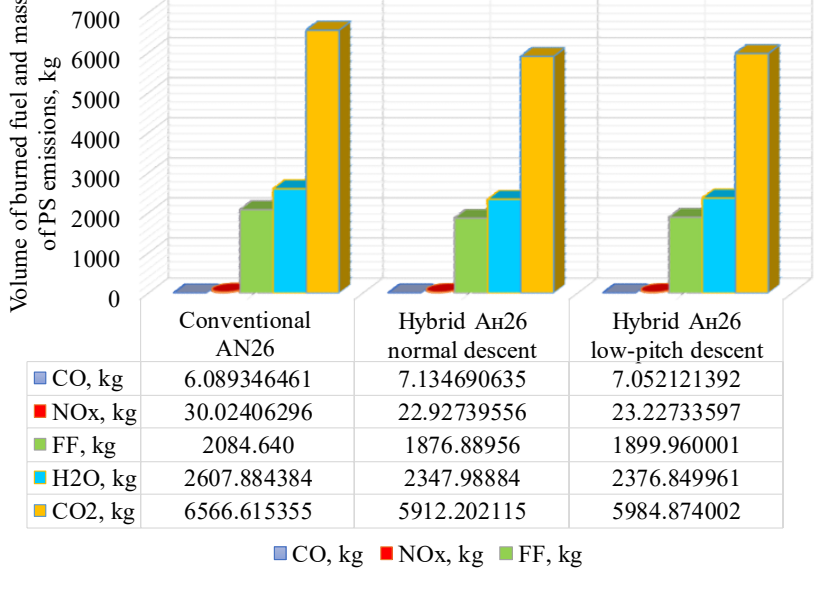

	Conventional AN26	Hybrid Ан26 normal descent	Hybrid Ан26 low-pitch descent
CO, kg	6.089346461	7.134690635	7.052121392
NOx, kg	30.02406296	22.92739556	23.22733597
FF, kg	2084.640	1876.88956	1899.960001
H2O, kg	2607.884384	2347.98884	2376.849961
CO2, kg	6566.615355	5912.202115	5984.874002

Fig. 11. Results of calculating the mass of fuel burned and the emissions of nitrogen oxides, carbon monoxide, carbon dioxide, and water vapor for the entire flight path (normal and with a low-pitch descent) for AN26 with a conventional and hybrid power plant

6. Discussion of results of modeling emission indices for conventional and hybrid aircraft

The improved module for calculating emission indices by combining the module for calculating the parameters of the flight path and the results of calculating the thermogas-dynamic calculation of the aircraft engine makes it possible to detect the influence of fuel consumption (engine thrust) on the values of emission indices. This feature is representative for evaluating the efficiency of hybrid engines because the electrification of the aircraft fleet is primarily aimed at reducing fuel consumption.

The analysis of our simulation results reveals that the fuel consumption and EINOx are significantly reduced (for the climb stage – 25 %; for the descent stage – 30 %) for the hybrid AN26 compared to the conventional AN26 (Fig. 9). The specified operational measure, in the part of a low-pitch descend, significantly reduces the EICO for the hybrid AN26 by an average of 50 % compared to the decrease stage for the conventional trajectory (Fig. 10). At the same time, the EICO values for the hybrid An26 for the trajectory with a low-pitch descent remain slightly higher than in the case of the conventional An26. The identified trend is due to the reduction of fuel consumption during the operation of the hybrid power plant, which leads to an increase in EICO, Fig. 10.

The results of the calculations for the entire flight path demonstrate that the use of a hybrid power plant for the An26 helps reduce fuel consumption by an average of 10 %, NOx emissions by 25 %, water vapor emissions by 10 %, and CO_2 by 10 % (Fig. 11).

It should be noted that the considered method does not allow determining the emissions of suspended particulate matter (PM_10, $PM_{2.5}$, $PM_{1.0}$), which are a priority, in particular, in terms of assessing local atmospheric air quality. In the future, it is planned to improve the presented module regarding the calculation of emissions of suspended particles and the integration of the calculated emission indices for modeling the concentrations of pollutants in the atmospheric air at the airport. It is also planned to carry out a sensitivity analysis of the considered module in order to determine the degree of dependence of the calculated emission indices on the initial parameters, namely fuel consumption, trajectory parameters, and meteorological conditions.

The electric motors in the hybrid PS were used only during the first 12 minutes of the flight. That made it possible to use a gas turbine engine with less power, since the most thrust is needed for the run-off and the start of the climb. Operational limitations when calculating the flight path were satisfied by changing the angle of attack and the mode of operation of the gas turbine and electric engines. For flight segments where such a change could not be selected manually, GA was used.

In the future, it is planned to build a trajectory model that will take into account the roll and movement of the aircraft in three-dimensional space for comparison with experimentally measured masses of pollutants.

7. Conclusions

1. A method for calculating the flight profile of an aircraft with a hybrid PS has been improved. The calculation of the flight trajectory showed an increase in the flight range of the An-26 with a hybrid PS by 11.7 % compared to the An-26 with a conventional PS, with a degree of hybridization at takeoff of 37.2 %.

2. The emission indices at ICAO certification points for an aircraft with a hybrid power plant (similar to the TV3-117VMA-SBM1 with reduced power by 10 %) based on the selected PW127A analog have been substantiated.

3. Modeling of aircraft emissions with conventional and hybrid power plants was carried out, taking into account real fuel consumption along the flight path based on an improved module for calculating emission indices. The use of a hybrid power plant for the An-26 helps reduce fuel consumption by an average of 10 %, NOx emissions – 25 %, water vapor emissions – 10 %, CO_2 – 10 %.

Conflicts of interest

The authors declare that they have no conflicts of interest in relation to the current study, including financial, personal, authorship, or any other, that could affect the study and the results reported in this paper.

Funding

Developed within the framework of applied research: development of methods for noise and emission of pollutants reduction of nationally manufactured regional aircraft with a hybrid power plant. State registration number 0122U001802.

Data availability

All data are available in the main text of the manuscript.

Use of artificial intelligence

The authors confirm that they did not use artificial intelligence technologies when creating the current work.

References

1. Zaporozhets, O., Isaienko, V., Synylo, K. (2021). PARE preliminary analysis of ACARE FlightPath 2050 environmental impact goals. CEAS Aeronautical Journal, 12 (3), 653–667. https://doi.org/10.1007/s13272-021-00525-7
2. Boeing Market Outlook (2018). Seattle.
3. Global Networks, Global Citizens. Global Market Forecast 2018-2037. Airbus. Available at: https://www.airbus.com/sites/g/files/jlcbta136/files/2021-07/Presentation-Eric-Schulz-GMF-2018.pdf
4. Effects of Novel Coronavirus (COVID-19) on Civil Aviation: Economic Impact Analysis. ICAO. Available at: https://www.icao.int/sustainability/Documents/COVID-19/ICAO_Coronavirus_Econ_Impact.pdf

5. ICAO Environmental Report 2022. ICAO. Available at: https://www.icao.int/environmental-protection/Pages/envrep2022.aspx
6. Flightpath 2050. Europe's Vision for Aviation. Report of the High Level Group on Aviation Research. Available at: https://www.arcs.aero/sites/default/files/downloads/Bericht_Flightpath_2050.pdf
7. Aviation Environmental Report 2022. Office of the European Union. https://doi.org/10.2822/04357
8. Doc 9889. Airport Air Quality (2011). ICAO.
9. Turbovintovoy dvigatel' TVZ-117VMA-SBM1. Rukovodstvo po tehnicheskoy ekspluatatsii. Kniga 3.
10. GRABIT. Available at: https://www.mathworks.com/matlabcentral/fileexchange/7173-grabit
11. Kim, B., Rachami, J. Aircraft Emissions Modeling under Low Power Conditions. Paper # 716. Available at: https://citeseerx.ist.psu.edu/document?repid=rep1&type=pdf&doi=4506739f2ff5d5d38b499f7ba39d37bf176e766f
12. Aircraft and Airport-Related Hazardous Air Pollutants: Research Needs and Analysis (2008). Transportation Research Board. https://doi.org/10.17226/14168
13. Madden, P., Park, K. (2003). Methodology for Predicting NOx Emissions at Altitude Conditions from Ground Level Engine Emissions and Performance Test Information. Technical Report DNS 90713.
14. Duchêne, N., Synylo, K., Carlier-Haouzi, S. (2011). Deliverable D1 – Validation Test Report, CS-GA-2009-255674-TURBOGAS. TURBOGAS Deliverable.
15. Tereshchenko, Yu. M., Kulyk, M. S., Mitrakhovych, M. M., Volianska, L. H. (2015). Teoriya teplovykh dvyhuniv. Hazodynamichnyi rozrakhunok elementiv hazoturbinnykh dvyhuniv. Kyiv: NAU, 292.
16. de Vries, R., Brown, M., Vos, R. (2019). Preliminary Sizing Method for Hybrid-Electric Distributed-Propulsion Aircraft. Journal of Aircraft, 56 (6), 2172–2188. https://doi.org/10.2514/1.c035388
17. Zaporozhets, O., Makarenko, V., Tokarev, V., Kazhan, K., Synylo, K. (2023). Modelling the noise characteristics of a regional turboprop hybrid-electric aircraft. International Symposium on Electric Aviation and Autonomous Systems. Warsaw. Available at: https://2023.iseasci.org